



RESEARCH ARTICLE

Low Field Magnetic Resonance Imaging Characteristics of Experimental Canine Intracranial Hemorrhage

Jimo Jeong¹, Yechan Jung^{1,2}, Eunseok Jeong¹, Youngkwon Cho³ and Kichang Lee^{*1}

¹Department of Veterinary Clinical Service, Chonbuk National University Specialized Campus: 79 Gobong-ro, Iksan-si, Jeollabuk-do 54596 Republic of Korea; ²Research Ethics Center Office of Research Management, Korea University, Seoul, 02841, Korea; ³College of health sciences, Radiologic science, Cheongju University, 298, Daesung-ro, Sandang-gu, Cheongju, 360-764 Republic of Korea

*Corresponding author: kclee@jbnu.ac.kr

ARTICLE HISTORY (16-010)

Received: January 21, 2016
Revised: January 24, 2017
Accepted: March 03, 2017
Published online: May 9, 2017

Key words:

Canine cerebral hemorrhages
Dog
Gradient echo sequences
Low field
Magnetic resonance
Signal

ABSTRACT

Magnetic resonance (MR) evaluation of intracranial hemorrhage is often challenging due to the variable appearance of hemorrhage, which depends on multiple factors. The aim of this study was to establish MR appearance of cerebral hemorrhages in dogs using low magnetic field and the efficacy of T2*-Gradient echo sequence for hemorrhage detection. Eight clinically normal beagle dogs, weighing approximately 9kg each were used. After a baseline MR examination, an intracranial hematoma was produced. MR examination was performed just after development of hemorrhage model and then at 1 to 2 day intervals for 30 days using low field MR (0.25 T). Sagittal images were acquired to select reproducible slice positions for transverse images. Sequences include spin echo (SE) T2, fluid attenuated inversion recovery (FLAIR), short tau inversion recovery, SE T1, and T2*-Gradient echo (GRE) images. The acquired MR images were compared subjectively to evaluate the signal changes. Signal-to-noise ratio was also measured and compared. Signal of the lesion was significantly hypo-intense in STIR and hyper-intense in T1W at day 3 after hemorrhage creation. The signal intensity of the hemorrhage gradually decreased in T1W images from day 3 to day 20. On T2W and FLAIR images, signal intensity was hyper-intense compared to normal and decreased gradually. No significant hypo-intense signal was seen on T2*-GRE image during examination of hemorrhage. This study shows that signal changes in intracranial hemorrhage do not follow the guidelines for hemorrhage interpretation in T1W and T2W images using low field magnets, except acute stage. T2*-GRE imaging maybe less useful in hemorrhage detection.

©2017 PVJ. All rights reserved

To Cite This Article: Jeong J, Jung Y, Jeong E, Cho Y and Lee K, 2017. Low field magnetic resonance imaging characteristics of experimental canine intracranial hemorrhage. *Pak Vet J*, 37(3): 316-320.

INTRODUCTION

There are multiple reports of the MR imaging features of intracranial hemorrhage in humans and in intracranial hemorrhagic animal models. These reports indicate that the appearance of intracranial hemorrhage on MR imaging depends primarily on the age of the hematoma and the type of MR sequence, such as T1 weighted (T1W) or T2 weighted (T2W) sequences (Bradley Jr, 1993). These reports also suggest five distinct stages of hemorrhage related to hemoglobin oxidation (Bradley Jr, 1993). Other reports using intracranial hemorrhagic animal models documented the effects of

various parameters including size of the lesion, source (arterial, venous), location (ventricular, epidural, subdural, parenchymal), time from onset, and field strength. They found that GRE imaging is highly useful in detecting and delineating hemorrhage with 0.6T and 1.5T magnets (Weingarten *et al.*, 1991; Jung *et al.*, 2015).

However, time-dependent evaluation of MR-imaging patterns has not yet been defined in dogs, especially using low magnetic fields. The aims of this study were to evaluate and define signal intensity changes in canine intracranial hemorrhage on T2W, T1W, FLAIR and STIR sequences, and to evaluate the ability of T2*-GRE sequences to detect hemorrhage using low magnetic fields.

MATERIALS AND METHODS

The study was conducted prospectively from November to December 2013. The treatment of the experimental animals was approved by the Institutional Animal Care and Use Committees (IACUC) of Chonbuk National University. Eight healthy female beagle dogs with a mean age of 6 years and a mean body weight of 9 kg were used to induce experimental intracranial hemorrhage. We performed a general and neurological examination and complete blood work prior to hemorrhage induction. A venous catheter was placed in the cephalic vein, general anesthesia was induced with the combination of medetomidine and tiletamine/zolazepam (combination of Tomidin® (Provet, Veterinary Products Ltd., Istanbul, Turkey) and Zoletil 50® (Virbac Laboratories, Carros, France), 0.02 ml/kg intravenously). After endotracheal intubation, anesthesia was maintained via 1.5-2% isoflurane (Hana Pharm. Co., Kyonggi-Do, South Korea) and oxygen. In creating a canine intracranial hemorrhage model, the single blood injection model was used as described previously (Manaenko *et al.*, 2011, Weingarten *et al.*, 1991). Using an aseptic technique, a burr hole was surgically created in the parietal bone, with care taken to avoid penetrating the dura mater. After the burr hole was cleaned, 2~3 ml of blood was collected from the femoral artery of each dog. This blood was immediately injected into the temporal lobe through the burr hole with a saline-filled 24-gauge needle at a depth of 2 cm from the inner calvaria. The needle was then removed, and the burr hole was covered with bone wax. (Fig. 1) Using autologous arterial blood, eight intracranial hemorrhages were successfully created. The percentage O₂ saturation and blood pH were measured using a Vet stat electrolyte and blood gas analyzer (IDEXX, Westbrook, Maine, USA). The Partial Thromboplastin time (PT) and Activated Partial Thromboplastin Time (APTT) were measured with a cassette-based coagulation analyzer (DX Coag, IDEXX Laboratories).

MR scanning was performed using a 0.25T (Vet Grande, Esaote, Italy) system and a solenoid knee coil. Five sequences were used to acquire images of the dog brains at 1-day intervals for 30 days. The sequences included transverse T2-weighted (T2W: turbo spin echo (4260/90; TR/TE)), T1-weighted (T1W: spin echo (860/18; TR/TE)), T2*-gradient echo (1105/22; TR/TE), fluid-attenuated inversion recovery (FLAIR) (7140/90/17500; TR/TE/IR), and short tau inversion recovery (STIR) (5250/80/120; TR/TE/IR). Acquisition parameters are shown in table 1. The slices were 3.5 mm thick for transverse plane images with a 0.4-mm gap. Digital Imaging and Communications in Medicine (DICOM) images of the dogs were acquired every day from day 0 to day 30. The signal intensity of lesion was subjectively graded as null, hypo-intense, isointense, or hyper-intense.

Homogeneity of signal intensity and size change were also evaluated. Three radiologists compared the DICOM images from days 0 to 30 side by side using PACS software (INFINITT Healthcare, Seoul, Korea) to assess visual differences in signal intensity. The readers subjectively chose the window width and level at which to view each sequence. The same width and level were used for each sequence to compare subsequent images from days 0 to 30.

Histopathologic examination was performed on formalin fixed brain tissue after day 30. Six micrometer section of each brain block were prepared, stained with hematoxylin and eosin and evaluated by light microscopy.

RESULTS

Hemorrhagic lesions less than 2cm*1cm were successfully created in 8 beagles and were located in the frontal and temporal lobe region. Hemorrhagic lesion was observed over 3 to 4 slices in the transverse plane MR images (Fig. 2 & 3). The subjective assessments of chronological MR characteristics of eight canine intracranial hemorrhages by three radiologists are summarized in table 2. There are slight differences in section plane between examinations of the same subject at different times. Initially, the lesions were hyper-intense in T2W images and hypo-intense in T1W images compared with the cerebral cortex in all subjects, and signal intensity was homogenous in all sequences. Between 1 and 3 days after creation, the lesion became partially hyper-intense in T1W images; the hyper-intense signal was sustained in T2W images, though signal intensity of hemorrhagic lesions subjectively decreased in all subjects. Initial mild T1 hyper-intensity observation time in T1W images differed between subjects. The development of partial T1 hyper-intensity in T1W images on day 3 in 6 subjects showed readily decreased SI, but two subjects showed increased SI until day 7. This hyper-intensity changed to iso-intensity or mild hyper-intensity in T1W images at day 21. Hemorrhagic lesions of all subjects showed decreased T2 hyper-intensity after day 1, and this hyper-intensity was sustained even though lesion size was decreased at 30 days (Fig. 4 & 5).

In FLAIR images, the lesions were initially homogenous and hyper-intense, with the hyper-intensity being sustained in FLAIR images during the study period until lesion size became focal at day 21 (Fig. 7). In STIR images, the hemorrhagic lesion was hyper-intense at day 1. Between 1 and 3 days, a partial hypo-intense to null signal developed in all subjects, indicating a significant heterogeneous signal pattern in STIR images (Fig. 6). No significant susceptibility artifact was visible in T2*-GRE images, but hyper-intensity was shown until lesion size became focal and difficult to detect at day 21 (Fig. 8).

After development of a partial T1 hyper-intense signal and STIR hypo-intense to null signal, hemorrhagic lesions had a heterogeneous signal intensity.

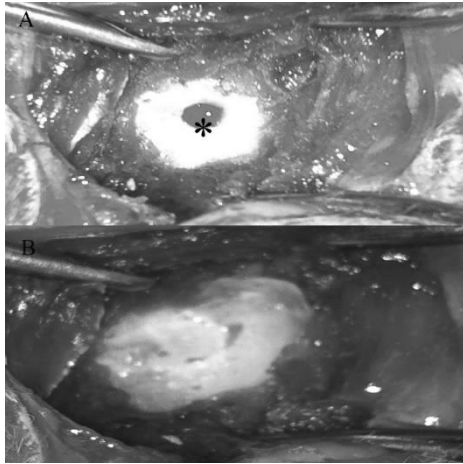
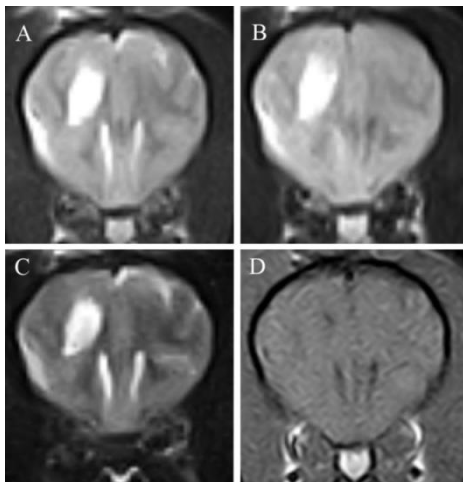
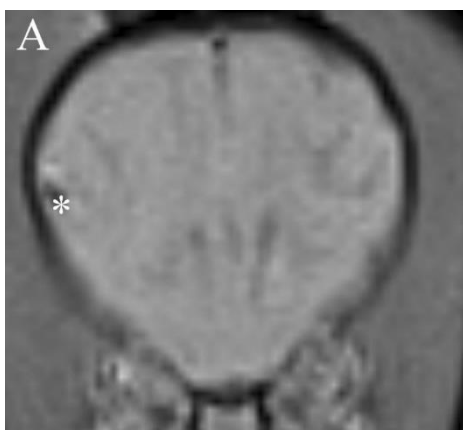
Table 1: Acquisition parameters for the Transverse imaging

Sequence	Plane	TR(ms)	TE(ms)	FOV(mm)	Matrix	Thickn (mm)	Flip (°)	NEX	TI
T2W	Trans	4260	90	200*200	288*192	3.5	90	1	
T1W	Trans	860	18	288*215	288*215	3.5	90	1	
FLAIR	Trans	7140	90	200*200	192*192	3.5	90	1	1750
STIR	Trans	5250	80	200*200	256*192	3.5	90	1	120
T2*-GRE	Trans	1105	22	200*200	256*192	3.5	40	1	

TR, repetition time; TE, echo time; FOV, field of view; Thickn, thickness; TA, acquisition time; NEX, number of acquisitions; TI, inversion time; TSE, turbo spin echo; STIR short tau inversion recovery.

Table 2: Summary of common findings in signal intensity changes of intracranial hemorrhage

Stage	Time	T1W	T2W	FLAIR	STIR	T2*-GRE
Hyperacute	(<24hr)	Iso	Hyper (mild heterogeneous)	Hyper	Hyper	Iso
Acute	(1~3day)	Mild Partail Hyper	Hyper (But decreased compared to day 0)	Hyper	Hyper + partial hypo	Hyper to iso
Early	(3+ days)	Partial Hyper	Hyper (But decreased compared to day 0)	Hyper	Hyper + partial hypo	Hyper to iso
Late	(7+ days)	Partial Hyper	Hyper (But decreased compared to day 0)	Hyper	Partial hypo	Hyper to iso
Late	(20+ days)	Hyper to Iso	Hyper (lesion size is decreased to focal)	Hyper	Hyper	Iso
Chronic	(21+ days)	Iso	Focal Hyper intense	Hyper	Hyper (mild heterogeneous)	Iso

**Fig. 1:** A) burr hole (*) on parietal bone B) covered with bone wax on burr hole after hemorrhage induction.**Fig. 2:** Transverse MR images of successfully induced intracranial hemorrhagic lesion on different sequences at Day 0. A) T2W B) FLAIR C) STIR D) T1W.**Fig. 3:** Transverse MR images of successfully induced intracranial hemorrhagic lesion on Day 0. A) T2*-GRE, the air introduction during surgery was seen in the lesion (asterisk).

Histopathologic results showed cerebral inflammation by RBC clot, hemosiderin in macrophages, formation of gitter cells, angiogenesis around the fibrin clot, and fibrotic scar formation. The histopathologic exam showed no significant correlation with MR imaging.

DISCUSSION

The MR appearance of canine intracranial hemorrhage with a 0.25T low-field magnet was presented in this study. The results of time changes in MR appearance of canine intracranial hemorrhage in low magnetic fields do not agree with prior descriptions (Weingarten *et al.*, 1991, Bradley Jr, 1993). Time-related changes on MR imaging of hyperacute to chronic hematomas have been used as criteria for selecting treatment in human medicine (Bradley Jr, 1993). There are only a few case reports regarding MR imaging features of intracranial hemorrhage in animals (Thomas *et al.*, 1997, Vernau *et al.*, 2002, Tamura *et al.*, 2006, Dennler *et al.*, 2007, Fulkerson *et al.*, 2012). These cases describe subacute hematomas associated with cerebral vascular malformation, hemorrhage within an arachnoid cyst, metastatic hemangiosarcoma causing cerebral hemorrhage, and cerebral microbleeds in four dogs (Thomas *et al.*, 1997, Vernau *et al.*, 2002, Dennler *et al.*, 2007, Fulkerson *et al.*, 2012). Only one case report describes sequential intracranial hematoma in a dog (Tamura *et al.*, 2006). In this report, the signal intensity changed to hyper-intense on T1-weighted images, while the center of the lesion changed to hypo-intense, then hyper-intense with a hypo-intense rim on T2-weighted images with a 0.2T permanent magnet because of hemoglobin oxidation in a dog with seizures (Tamura *et al.*, 2006).

An *in vivo* canine animal model was believed to be an ideal method for studying intracranial hemorrhage because the precise time from hemorrhage to MR imaging could be determined (Weingarten *et al.*, 1991). Theoretically, the source, size, and location of the hematoma can be closely controlled (Weingarten *et al.*, 1991). The induced hemorrhagic lesions in eight dogs had slightly different shapes, sizes, and distributions. Prior reports stated that variability in hematoma size was impossible to control, as dissection of blood along the injection tract is a significant limitation in this animal model (Weingarten *et al.*, 1991). In our experience, this is because the volume of backdraft in the blood injection at induction was slightly different in each experiment. The induced hemorrhagic lesion was distributed in the temporal to frontal lobes. This wide distribution is another limitation of animal models. To avoid influence of blood source, autologous femoral arterial blood was used for hemorrhage induction.

All animals initially showed ipsilateral strabismus and stuporous mental status; however, after 3 days of induction, they recovered normal mental status and showed normal physical condition until the end of the study period.

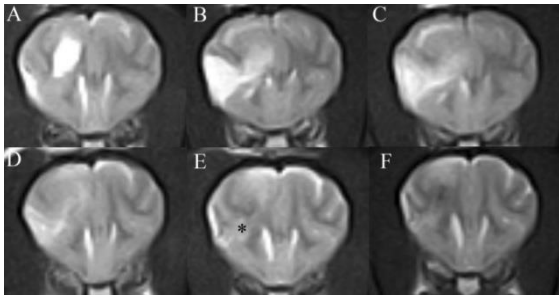


Fig. 4: Serial T2W images. A) 1hr B) Day 1 C) Day 3 D) Day 10 E) Day 21 *Note The hemorrhagic lesion is almost disappeared. F) Day 29.

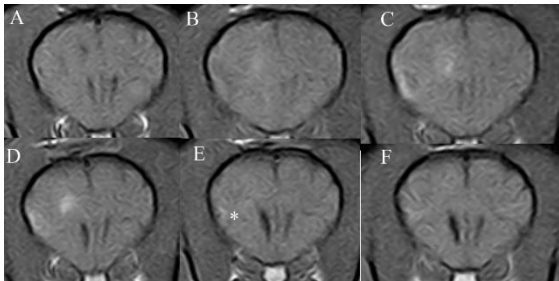


Fig. 5: Serial T1W images. A) 1hr B) Day 1 C) Day 3 * Note significant T1 hyper intensity was visible. D) Day 10 E) Day 25 *The hemorrhagic lesion is almost disappeared. F) Day 29.

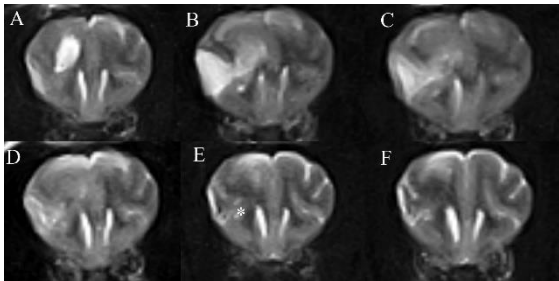


Fig. 6: Serial STIR images. A) 1hr B) Day 1 C) Day 3 * Note hyper intensity was visible. D) Day 10 E) Day 25 * The hemorrhagic lesion was almost disappeared. F) Day 29.

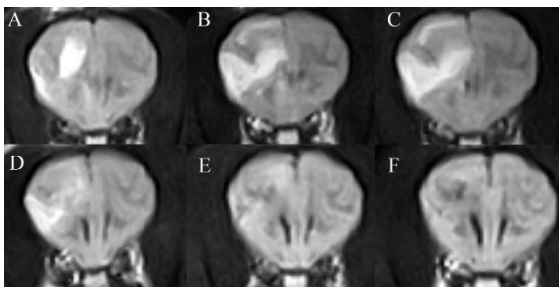


Fig. 7: Serial FLAIR images. A) 1hr B) Day 1 C) Day 3 D) Day 10 E) Day 25 F) Day 29.

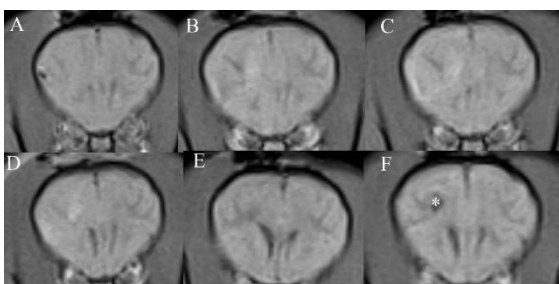


Fig. 8: Serial T2*-GRE images. A) 1hr B) Day 1 C) Day 3 D) Day 10 E) Day 25 F) Day 29 * hypo intensity was not seemed to be susceptibility artifact, because this lesion was appeared hypo intensity on T1W, FLAIR sequences.

During days 1-3, signal intensity changes in the hemorrhagic lesion in T2W and T1W images were similar to prior reports of the acute stage. (Thomas *et al.*, 1997, Vernau *et al.*, 2002, Tamura *et al.*, 2006, Dennler *et al.*, 2007, Fulkerson *et al.*, 2012). However, hyper-intensity in T2W images readily decreased after day 1, while hyper-intensity compared to the adjacent cerebral cortex was sustained until lesion detection became difficult as the lesion size became focal. The developed partial hyper-intensity in T1W images readily decreased but was sustained until lesion detection became impossible around day 21. This suggests that no significant stage discrimination in intracranial hemorrhage was visible in vivo. We believe that prior descriptions of five stages of hemorrhage are theoretical based on hemoglobin degradation. Using hyper-intensity in T1W images for hemorrhage detection might be very useful until 21 days after onset.

On T2W images, the hemorrhagic lesion changed to a mild hypo-intense state after day 1, so the signal pattern became mildly heterogeneous. Because the partial SI change was mild, it was still hyper-intense compared to the adjacent cerebral cortex. Prior reports described that diminished development of hypo-intensity was observed with a 0.6T magnetic field compared with a 1.5T magnetic field (Weingarten *et al.*, 1991). These hypo-intensities in T2W images of acute hematoma can be explained by multiple hypotheses. Paramagnetic deoxy-hemoglobin may accumulate within the relatively hypoxic hematoma center. Hemoconcentration, clot formation, and retraction and diminution of RBC volume all may produce T2 shortening. A case report that performed sequential MR imaging in a dog with intracranial hematoma observed that the SI in T2WI changed from hypo-intense to hyper-intense at 7~10 days after onset (Tamura *et al.*, 2006). That, however, was not observed in our study.

The partial signal change was an unexpected finding. Hypo-intense to null signals was seen in STIR sequences at day 3, which corresponds to hyper-intense signal changes in T1W images. These signal changes were explainable with T1 time shortening of met-hemoglobin (Dürr *et al.*, 1997, Pang *et al.*, 2010). Human studies have revealed that time-related changes in SI always occur at the edge of the mass and spread toward the center (Brooks *et al.*, 1989; Bradley Jr, 1993). A veterinary case report involving a dog also showed central SI change in hematoma (Tamura *et al.*, 2006). However, partial SI changes in T1WI, T2WI, and STIR images did not define characteristics of chronological MR changes in intracranial hemorrhage. This might be the main cause of conflicting descriptions of time-related SI changes on MR images of hemorrhage.

FLAIR images have high sensitivity for several brain diseases in human beings and animals (Hajnal *et al.*, 1992, Kates *et al.*, 1996, Falzone *et al.*, 2008). FLAIR is considered to be a routine brain MR protocol (Noguchi *et al.* 1997, Bakshi *et al.* 1999, Linfante *et al.* 1999, Stuckey *et al.* 2007; Cherubini *et al.*, 2008). FLAIR images show hyper-intensity in hemorrhagic lesions. There are several hypotheses regarding these hyper-intense signals, and one of them is related to the role of protein in the blood (Bakshi *et al.*, 1999). The FLAIR technique produces strong T2WI that are highly sensitive to T2 prolongation

in tissue, likely resulting from high protein content (Bradley Jr, 1993, Melhem *et al.*, 1997).

STIR is a fat-suppressing technique with high sensitivity, low signal to noise ratio, excellent gray/ white matter contrast (Konar *et al.*, 2011). STIR images showed partial hypo- to null signal at 1~3 days, which is consistent with partial hyper-intensity in T1W images. Because of deoxy- and met-Hb conversion, T1 time shortening occurred in a similar pattern to that of Fat T1 time (Dürr *et al.*, 1997, Pang *et al.*, 2010). This is assumed to suppress the signal intensity in STIR images. In this work, the suppressed signal intensity change of hemorrhagic lesion was sustained until lesion size became focal.

Around 21 days, lesion detection became difficult because lesion size changed to focal in T2W, T1W, and T2*-GRE images. However, the lesion was still detectable in FLAIR and STIR images due to better lesion detection, which coincides with prior reports (Bakshi *et al.*, 1999; Hermier *et al.* 2001; Kato *et al.* 2002; Hiwatashi *et al.* 2003; Tsushima *et al.* 2003; Young *et al.*, 2015).

Contrary to prior reports, it can be difficult to detect hemorrhages with low magnetic fields (Thomas *et al.*, 1997, Vernau *et al.*, 2002, Dennler *et al.*, 2007, Fulkerson *et al.*, 2012, Lowrie *et al.*, 2012). Hemorrhagic lesions in T2*-GRE showed hyper-intensity compared to the cerebral cortex in the present study. In human medicine, T2*-GRE sequences showed susceptibility artifacts of hemorrhagic lesions in both 1.5T magnetic fields and 0.6T magnetic fields (Weingarten *et al.*, 1991). This contradiction was unexpected, so in our work, we changed the sequence parameters during the study period in order to enhance the susceptibility artifact; however, this attempt was unsuccessful. This may be because susceptibility effects are weaker at low field than at high field (Konar *et al.*, 2011). This difference might also be a limitation of a 0.25T low magnetic field. Hemorrhage detection on T2*-GRE in a 0.25T low magnetic field may not be feasible compared to detection in a high field. The relationship between histopathologic and imaging changes is still unclear. It is uncertain whether there is a direct correlation between severity of histopathologic changes and MR signal. Further studies are needed to determine a specific relationship.

Conclusions: This study suggests a partial signal intensity change in T1W and T2W sequences was consistent with signal intensity change in the acute stage in previous reports. Except in the acute stage, there was no significant discrimination of stages with time in this study. T2*- GRE sequence imaging in hemorrhagic lesion was less useful in this study, especially with a 0.25T low field. This result increases the understanding of chronological low-field MR characteristics of canine intracranial hemorrhage caused by traumatic or vascular disease and provides guidelines for MR interpretation of hemorrhage with time in low magnetic fields.

Authors contribution: KL and JJ contributed to design the entire experiment. JJ, YJ and JE executed the experiment. JJ, KL and YC participated in image analysis, count rate calculation, and statistical analysis. All authors interpreted the data, critically revised the manuscript for important intellectual contents, approved the final version and agreed to publication.

Acknowledgements: This research was supported by Basic Science Research Program through the National Research Foundation of Korea (NRF), funded by the Ministry of Education (NRF2013R1A1A4AO1007690).

REFERENCES

- Bakshi R, Kamran S, Kinkel PR, *et al.*, 1999. Fluid-attenuated inversion-recovery MR imaging in acute and subacute, cerebral intraventricular hemorrhage. *AJNR Am J Neuroradiol* 20:629-36.
- Bradley Jr WG, 1993. MR appearance of hemorrhage in the brain. *Radiology* 189:15-26.
- Cherubini G, Platt S, Howson S, *et al.*, 2008. Comparison of magnetic resonance imaging sequences in dogs with multi-focal intracranial disease. *J Small Anim Prac* 49:634-40.
- Dennler M, Lange E, Schmied O, *et al.*, 2007. Imaging diagnosis metastatic hemangiosarcoma causing cerebral hemorrhage in a dog. *Vet Radiol Ultrasound* 48:138-40.
- Hajnal JV, De Coene B, Lewis PD, *et al.*, 1992. High signal regions in normal white matter shown by heavily T2- weighted CSF nulled IR sequences. *J Comput Assist Tomogr* 16:506-13.
- Hermier M, Nighoghossian N, Derex L, *et al.*, 2001. MRI of acute post-ischemic cerebral hemorrhage in stroke patients: diagnosis with T2-weighted gradient-echo sequences. *Neuroradiol* 43:809-15.
- Hiwatashi A, Kinoshita T, Moritani T, *et al.*, 2003. Hypointensity on diffusion-weighted MRI of the brain related to T2 shortening and susceptibility effects. *Am J Roentgenol* 181:1705-709.
- Jung Y, Jeong J, Park S, *et al.*, 2015. Low-field magnetic resonance imaging feature of severe chronic fetlock injury in a horse. *Pak Vet J* 35:131-3.
- Kates R, Atkinson D and Brant-Zawadzki M, 1996. Fluid-attenuated inversion recovery (FLAIR): clinical prospectus of current and future applications. *Top Magn Reson Imaging* 8:389-96.
- Kato H, Izumiyama M, Izumiyama K, *et al.*, 2002. Silent cerebral microbleeds on T2*-weighted MRI. *Stroke* 33:1536-540.
- Konar M and Lang J, 2011. Pros and cons of low-field magnetic resonance imaging in veterinary practice. *Vet Radiol Ultrasound* 52:S5-S14.
- Linfante I, Llinas RH, Caplan LR, *et al.*, 1999. MRI features of intracerebral hemorrhage within 2 hours from symptom onset. *Stroke* 30:2263-267.
- Lowrie M, De Risio L, Dennis R, *et al.*, 2012. Concurrent medical conditions and long-term outcome in dogs with nontraumatic intracranial hemorrhage. *Vet Radiol Ultrasound* 53:381-8.
- Manaenko A, Chen H, Zhang JH, 2011. Comparison of different preclinical models of intracerebral hemorrhage. *Acta Neurochir Suppl* 111:9-14.
- Melhem ER, Jara H and Eustace S, 1997. Fluid-attenuated inversion recovery MR imaging: identification of protein concentration thresholds for CSF hyperintensity. *AJR Am J Roentgenol* 169:859-62.
- Noguchi K, Ogawa T, Seto H, *et al.*, 1997. Subacute and chronic subarachnoid hemorrhage: diagnosis with fluid-attenuated inversion-recovery MR imaging. *Radiology* 203:257-62.
- Pang KK, Tsai YS, Chang HC, 2010. Methemoglobin suppression in a 0.3 Tesla magnet: an in vitro and in vivo study. *Acad Radiol*, 17: 624-7.
- Stuckey SL, Goh TD, Heffernan T, *et al.*, 2007. Hyperintensity in the subarachnoid space on FLAIR MRI. *Am J Roentgenol* 189:913-21.
- Tamura S, Tamura Y, Tsuka T, *et al.*, 2006. Sequential magnetic resonance imaging of an intracranial hematoma in a dog. *Vet Radiol Ultrasound* 47:142-4.
- Thomas WB, Adams WH, McGavin MD, *et al.*, 1997. Magnetic resonance imaging appearance of intracranial hemorrhage secondary to cerebral vascular malformation in a dog. *Vet Radiol Ultrasound* 38:371-5.
- Tsushima Y, Aoki J, Endo K, 2003. Brain microhemorrhages detected on T2*-weighted gradient-Echo MR images. *Am J Neuroradiol* 24:88-96.
- Vernau KM, LeCouteur RA, Sturges BK, *et al.*, 2002. Intracranial intracranial cyst with intracystic hemorrhage in two dogs. *Vet Radiol Ultrasound* 43:449-54.
- Weingarten K, Zimmerman R, Deo-Narine V, *et al.*, 1991. MR imaging of acute intracranial hemorrhage: findings on sequential spin-echo and gradient-echo images in a dog model. *Am J Neuroradiol* 12:457-67.
- Young BD, Mankin JM, Griffin JF, *et al.*, 2015. Comparison of two fat-suppressed magnetic resonance imaging pulse sequences to standard t2- weighted images for brain parenchymal contrast and lesion detection in dogs with inflammatory intracranial disease. *Vet Radiol Ultrasound* 56:204-11.